Journal of Sound and Vibration (2000) **229**(4), 775–792
doi:10.1006/jsvi.1999.2397, available online at http://www.idealibrary.com on IDEAL®

PERIODIC FORCED RESPONSE OF STRUCTURES HAVING THREE-DIMENSIONAL FRICTIONAL CONSTRAINTS

J. J. CHEN, B. D. YANG AND C. H. MENQ

Coordinate Metrology and Measurement Laboratory, Department of Mechanical Engineering, The Ohio State University, Columbus, OH 43210, *U.S.A.*

(*Received* 30 *November* 1998, *and in final form* 21 *May* 1999)

Many mechanical systems have moving components that are mutually constrained through frictional contacts. When subjected to cyclic excitations, a contact interface may undergo constant changes among sticks, slips and separations, which leads to very complex contact kinematics. In this paper, a 3-D friction contact model is employed to predict the periodic forced response of structures having 3-D frictional constraints. Analytical criteria based on this friction contact model are used to determine the transitions among sticks, slips and separations of the friction contact, and subsequently the constrained force which consists of the induced stick–slip friction force on the contact plane and the contact normal load. The resulting constrained force is often a periodic function and can be considered as a feedback force that influences the response of the constrained structures. By using the Multi-Harmonic Balance Method along with Fast Fourier Transform, the constrained force can be integrated with the receptance of the structures so as to calculate the forced response of the constrained structures. It results in a set of non-linear algebraic equations that can be solved iteratively to yield the relative motion as well as the constrained force at the friction contact. This method is used to predict the periodic response of a frictionally constrained 3-d.o.f. oscillator. The predicted results are compared with those of the direct time integration method so as to validate the proposed method. In addition, the effect of super-harmonic components on the resonant response and jump phenomenon is examined.

1. INTRODUCTION

Many mechanical systems have moving components that are mutually constrained through frictional contacts. When subjected to cyclic excitations, a contact interface may undergo constant changes among sticks, slips and separations, which lead to very complex contact kinematics. In previous studies of dry friction damper systems, according to the Coulomb friction law, the friction coefficient at the contact interface is usually assumed to be constant, the relative motion across the friction contact point is often one-dimensional, and the system is subjected to constant normal load [1]. It usually results in very simple contact kinematics and

0022-460X/00/040775 + 18 $35.00/0

can be used to obtain analytical solutions for single-degree-of-freedom systems [2, 3]. It can also integrate with the Multi-Harmonic Balance Method to yield approximate solutions for single-degree-of-freedom systems [4–6] and multiple-degree-of-freedom systems [7–9]. It was shown by Menq *et al.* [10] that the normal load across the friction contact point may vary dynamically with the vibratory motion of a single-degree-of-freedom system, and causes the contact point to stick, slip and possibly separate. A two-dimensional friction contact model that characterizes the transitions among sticks, slips and separations of the contact interface was recently proposed by Yang and Menq [11]. In this study, analytical criteria were developed to predict the transitions among sticks, slips and separations of friction contact interface.

In order to characterize the three-dimensional contact kinematics of a friction contact, Yang and Menq [12] proposed a three-dimensional friction contact model and developed analytical criteria to predict the transitions among sticks, slips and separations of the friction contact when the resulting relative motion is three-dimensional. These analytical criteria were employed to simulate the hysteresis loop for a given relative motion at the contact interface, so as to characterize the equivalent friction damping and non-linear stiffness induced by the friction constraint. They were integrated with the single-term Harmonic Balance Method to predict the resonant response of a frictionally constrained three-degrees-of-freedom oscillator. Since the single-term Harmonic Balance Method was used, the effect of the super-harmonic components of the constrained force on the structure's vibration was ignored. In addition, the resulting relative motion at the friction contact is assumed to be harmonic. Since the actual relative motion often has super-harmonic components, this assumption hinders accurate predictions of the transitions among sticks, slips and separations of the friction contact.

In this paper, a 3-D friction contact model [12] is employed to predict the periodic forced response of structures having 3-D frictional constraints. In the friction contact model, a contact plane is defined and its orientation is assumed invariant. The resulting relative motion across the two contacting surfaces can be decomposed into two components: in-plane tangential motion on the contact plane and normal component perpendicular to the plane. The in-plane tangential relative motion is often two-dimensional, and it induces stick–slip friction. The normal relative motion can cause variation of the contact normal load and possible separation of the two contacting surfaces. Analytical criteria based on this friction contact model are used to determine the transitions among sticks, slips and separations of the friction contact, and subsequently the constrained force which consists of the induced stick–slip friction force on the contact plane and the contact normal load. The resulting constrained force is often a periodic function and can be considered as a feedback force that influences the response of the constrained structures. By using the Multi-Harmonic Balance Method along with Fast Fourier Transform, the constrained force can be integrated with the receptance of the structures so as to calculate the forced response of the constrained structures. It results in a set of non-linear algebraic equations that can be solved iteratively to yield the relative motion as well as the constrained force at the friction contact. This

method is used to predict the periodic response of a frictionally constrained 3-d.o.f. oscillator. The predicted results are compared with those of the direct time integration method so as to validate the proposed method. In addition, the effect of super-harmonic components on the resonant response and jump phenomenon is examined.

2. 3-D CONTACT KINEMATICS

When two vibrating bodies are mutually constrained by a friction contact, as shown in Figure 1, the periodic relative motion across the two contacting surfaces is usually three-dimensional, and is often not parallel to the contact plane. In order to analyze the induced stick–slip friction, the periodic relative motion in the 3-D space can be decomposed into an in-plane periodic motion on the contact plane and a periodically varying component normal to the contact plane. The in-plane periodic motion can induce stick–slip friction, and thus can attenuate the resonant response of the constrained mechanical systems. On the other hand, the normal component tends to alter the normal load across the interface; and this effect, in extreme circumstances, may lead to a separation of the interface. It should be noted that the variable normal load is taken as the sum of the initial contact force at equilibrium plus a term that is proportional to the periodically varying normal component of the relative motion.

In the 3-D contact model proposed by Yang and Menq [12], the contact interface between two vibrating bodies can be modelled as a substructure that contains a massless elastic element and a friction contact point, as depicted in Figure 2. In this model, the elastic element accounts for the shear and normal

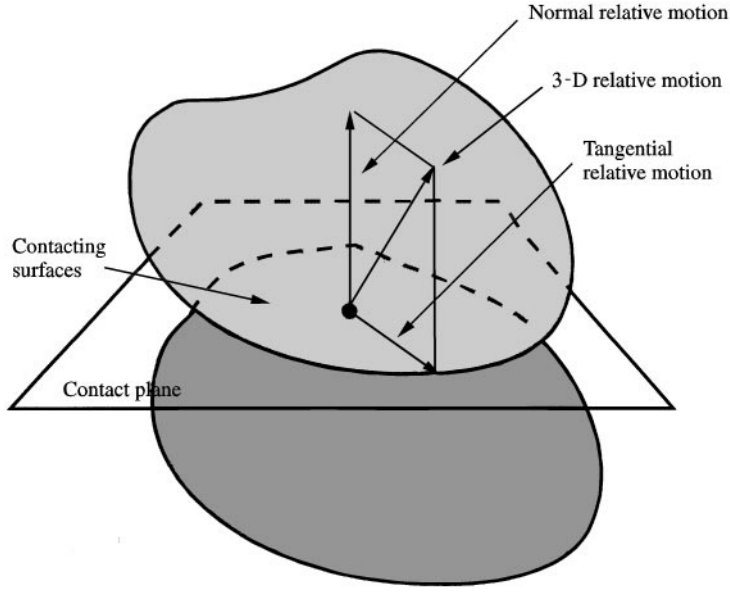

Figure 1. 3-D contact kinematics.

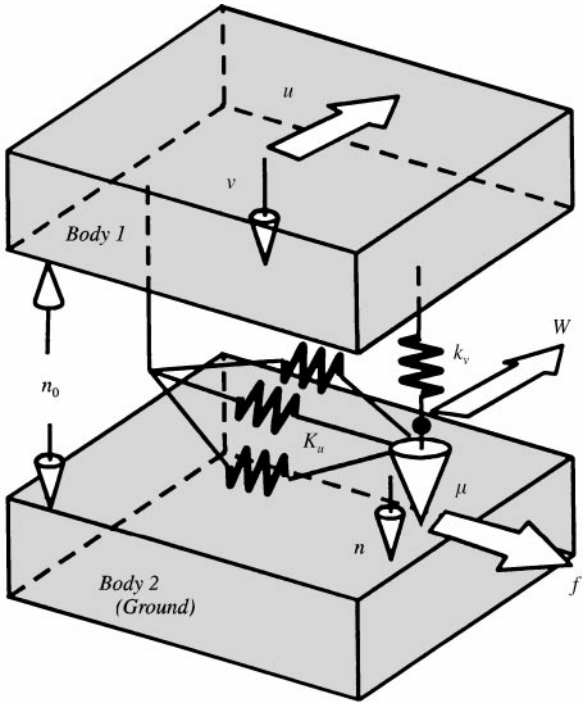

Figure 2. A model of the friction interface experiencing 3-D contact kinematics.

stiffness of the interface. It is characterized by a 2×2 stiffness matrix, $\mathbf{K_u}$, for the shear stiffness and a spring contact, k_v, for the normal stiffness. The friction contact point, that is assumed to obey the Coulomb friction law with the friction coefficient μ when in contact with *Body 2*, can undergo tangential stick–slip motion, and may experience intermittent separation from *Body 2* when the normal relative motion (v) becomes large. The contact interface is assumed to have either a preload or an initial gap (as designated by n_0). This model allows a negative preload to represent the situation when the interface has an initial gap; the equivalent preload to represent the situation when the interface has an initial gap; the equivalent preload across the interface with a gap e is calculated as $-k_v e$. In this model, $\mathbf{u}$ and v are the input tangential relative motion and normal relative motion of the contact interface, respectively, and they can be evaluated as the motion of *Body 1* with respect to *Body 2*. In this model, the 2×2 shear stiffness matrix $\mathbf{K_u}$ is used because the tangential relative motion is two-dimensional. If the shear stiffness property is isotropic, a spring constant k_u can be used, and the 2×2 shear stiffness matrix becomes $k_u\mathbf{I}$, in which $\mathbf{I}$ is the 2×2 identity matrix.

2.1. CONSTRAINED FORCE

The constrained force consists of two components: the induced stick–slip friction on the contact plane and the variable normal force. Since the friction force is

completely characterized by the relative motion, it will not lose generality to assume one of the contacting surfaces is the ground. With this assumption, the input tangential relative motion **u**, the slip motion of the contact point **w**, and the induced stick–slip friction **f** are vectors parallel to the ground; the normal relative motion v and the normal load n are scalars. The friction force, acting on the ground, can be expressed as

$$\mathbf{f} = \mathbf{K}_{\mathbf{u}}(\mathbf{u} - \mathbf{w}). \tag{1}$$

The normal load is taken as the sum of the preload n_0 plus the variation caused by v, and it can be expressed as

$$n = \begin{cases} n_0 + k_v v, & \text{when } v \geqslant -n_0/k_v, \\ 0, & \text{when } v < -n_0/k_v, \end{cases} \tag{2}$$

This friction contact model can be applied to the most general 3-D friction contact problem, where the orientation of the contact plane may oscillate when the structure vibrates. However, in this paper, we limit its applications to the case, in which the orientation of the contact plane can be assumed to be invariant. In many mechanical systems, this assumption is reasonable if the amplitude of vibration is relatively small when compared to the overall dimension of the structure.

2.2. STICK, SLIP AND SEPARATION

Depending on the amplitude and phase of the various components of the vibratory motion, the friction contact may either stick, slip or separate during a cycle of oscillation. When the vibratory motion is really small, the contact point sticks and the friction force is proportional to the displacement **u** with reference to $\dot{\mathbf{w}} = \mathbf{0}$, as implied in equation (1). According to the Coulomb friction law, the induced stick–slip friction is always limited to the varying slip load μn. During the course of the vibration, the interface may reach a point where the friction force tends to exceed the slip load and begins to slip. Subsequently, the friction force remains equal to the slip load, and slip takes place along the direction of the friction force until the contact point sticks again. In other words, the stick and slip conditions can be expressed as follows.

$$\text{Stick-state: } |\mathbf{f} - \mathbf{K}_{\mathbf{u}}(\mathbf{u} - \mathbf{u}_0) + \mathbf{f}_0| < \mu n, \quad \dot{\mathbf{w}} = \mathbf{0}, \tag{3}$$

$$\text{Slip-state: } \mathbf{f} = \mu n \frac{\dot{\mathbf{w}}}{|\dot{\mathbf{w}}|}, \quad \dot{w} \neq \mathbf{0}, \tag{4}$$

where $\mathbf{u}_0$ and $\mathbf{f}_0$ are the initial values of **u** and **f** at the beginning of the stick state. During the cycle of motion, the applied variable normal load may vanish to cause the interface to separate; consequently, the friction force is not present.

2.3. STICK/SLIP/SEPARATION TRANSITION CRITERIA

In order to evaluate the resulting periodic constrained force at the friction contact, analytical criteria are developed to determine the transitions among sticks, slips and separations, when experiencing variable normal load [12]. The analytical criteria can be summarized as follows.

(1) Stick-to-slip transition. This transition occurs when the friction force on the tangential plane reaches the varying slip load μn. That is,

$$|\mathbf{f} - \mathbf{K}_u(\mathbf{u} - \mathbf{u}_0) + \mathbf{f}_0| = \mu n. \tag{5}$$

To ensure that the magnitude of the friction force has a tendency to exceed the slip load, the following constraint is imposed:

$$|\dot{\mathbf{f}}| > \mu \dot{n}. \tag{6}$$

(2) Slip-to-stick transition. During the slip state, according to the Coulomb friction law, it was shown in reference [12] that the friction force can be solved from an initial value problem:

$$\dot{\mathbf{f}} = \mathbf{K}_u\left(\dot{\mathbf{u}} - \frac{\mathbf{f}^T\mathbf{K}_u\dot{\mathbf{u}} - \mu^2 n\dot{n}}{\mathbf{f}^T\mathbf{K}_u\mathbf{f}}\mathbf{f}\right). \tag{7}$$

The slip-to-stick transition occurs when the velocity of the relative motion $\dot{\mathbf{w}}$ equals 0, which implies

$$\mathbf{f}^T\mathbf{K}_u\dot{\mathbf{u}} - \mu^2 n\dot{n} = 0. \tag{8}$$

Since the initial friction force at the beginning of the slip condition is known, the initial value problem of equation (7) can be solved by using a numerical integration scheme such as the fourth order Runge–Kutta method to obtain the friction force $\mathbf{f}$. Once the friction force is obtained, the criterion of equation (8) can be used to predict the occurrence of the slip-to-stick transition.

(3) Stick/slip-to-separation transition. The transition from stick/slip to separation occurs when the normal load vanishes. In addition, the normal load should decrease at this moment to ensure the occurrence of the separation. Hence, the transition criteria can be formulated as

$$n = 0, \quad \dot{n} < 0. \tag{9}$$

(4) Separation-to-stick/slip transition. Similarly, the separation ends when the normal load is about to develop on the contact plane. Therefore, the moment of this transition can be determined by the criterion

$$n = 0, \quad \dot{n} \geqslant 0. \tag{10}$$

When the normal load and the friction force begin to develop on the contact plane at the end of the separation, their rate of change at the moment determine whether the following state is either stick or slip:

$$\dot{\mathbf{u}}^{\mathrm{T}}\mathbf{K}_{\mathbf{u}}^{\mathrm{T}}\mathbf{K}_{\mathbf{u}}\dot{\mathbf{u}} < \mu^2\dot{n}^2 \Rightarrow \text{Stick begins}, \tag{11}$$

$$\dot{\mathbf{u}}^{\mathrm{T}}\mathbf{K}_{\mathbf{u}}^{\mathrm{T}}\mathbf{K}_{\mathbf{u}}\dot{\mathbf{u}} \geqslant \mu^2\dot{n}^2 \Rightarrow \text{Slip beings}. \tag{12}$$

It should be pointed out that the incipient slip condition is regarded as an one-dimensional case, because the friction force is not present at this moment and the slip action will be developed along $\dot{\mathbf{u}}$. Thus, according to the Coulomb friction law, the rate of change of the developing friction force can be expressed as

$$\dot{\mathbf{f}} = \mu\dot{n}\frac{\dot{\mathbf{u}}}{|\dot{\mathbf{u}}|}. \tag{13}$$

Once the friction force develops, it can be further determined by solving the initial value problem of equation (7).

In this paper, these criteria are used to simulate hysteresis loops of the friction contact, when experiencing periodic relative motions. With these hysteresis loops, the constrained force can be linked to the relative motion between two contacting bodies. By using Fast Fourier Transform, the constrained force can be approximated by a series of harmonic functions and employed in the Multi-Harmonic Balance Method to predict the periodic response.

3. MULTI-HARMONIC BALANCE METHOD

The equation of motion for a structure experiencing three-dimensional frictional constraints under external periodic excitations can be expressed as

$$\mathbf{M}\ddot{\mathbf{U}}(t) + \mathbf{C}\dot{\mathbf{U}}(t) + \mathbf{K}\mathbf{U}(t) = \mathbf{f}_e(t) - \mathbf{f}_N(\mathbf{U}, \dot{\mathbf{U}}, t), \tag{14}$$

where $\mathbf{U}$ is the nodal displacement vector, $\mathbf{M}$ the mass matrix, $\mathbf{C}$ the damping matrix, $\mathbf{K}$ the stiffness matrix, $\mathbf{f}_e$ the external periodic excitation, and $\mathbf{f}_N$ the non-linear constrained force, which is a function of the motion at the contact point. The model is three-dimensional. If the model contains n nodes, all the matrices are $3n \times 3n$ matrices, and all the vectors have $3n$ elements.

The external periodic excitation can be resolved into a Fourier series:

$$\mathbf{f}_e = \sum_{k=1}^{\infty} \mathbf{f}_k^e \mathrm{e}^{\mathrm{j}k\omega t}, \tag{15}$$

in which ω is the fundamental frequency of the excitation force, and $\mathbf{f}_k^e$ represents the magnitude and the phase of its kth harmonic component. In the following analysis, the external periodic excitation is approximated as

$$\mathbf{f}_e \cong \sum_{k=1}^{m} \mathbf{f}_k^e \mathrm{e}^{\mathrm{j}k\omega t}, \tag{16}$$

where m is the number of harmonic components considered in the analysis. From linear vibration theory, without non-linear constrained force, the forced response of the structure due to external periodic excitation can be obtained by standard harmonic analysis. The complex receptance matrix corresponding to the kth harmonic frequency can be expressed as

$$\mathbf{R}_k = [\mathbf{r}_{il,k}] = [\mathbf{K} - (k\omega)^2\mathbf{M} + \mathrm{j}(k\omega)\mathbf{C}]^{-1}, \tag{17}$$

where $r_{il,k}$ is defined as the harmonic steady state response of the ith node due to the kth unit harmonic excitation force at the lth node.

Assume that there are p friction contact points. For simplicity, these contact points are assigned to be the first p nodes of the model. Therefore, the displacement vector of these friction contact points is expressed as

$$\mathbf{U}_c = [\mathbf{u}_i], \quad i = 1, 2, \ldots, p. \tag{18}$$

Since the external excitation is periodic, the steady state response and the induced constrained force are assumed to be periodic. The steady state periodic response at the ith node can be expressed as[†]

$$\mathbf{u}_i = \sum_{k=0}^{nl} \mathbf{u}_{i,k} \mathrm{e}^{\mathrm{j}k\omega t}. \tag{19}$$

The steady response at each node consists of two components. The first one is due to the external excitation force while the second component caused by the constrained forces at the friction contact points.

With the complex receptance matrix, the kth harmonic component of the steady state response at the ith node due to the external excitation force can be obtained as

$$\mathbf{u}_{i,k}^e = \sum_{l=1}^{n} \mathbf{r}_{il,k}\, \mathbf{f}_{l,k}^e, \tag{20}$$

where $\mathbf{u}_{i,k}^e$ is the kth harmonic response of the ith node due to the external excitation and $\mathbf{f}_{l,k}^e$ is the kth harmonic component of the external excitation at the lth node.

[†] In order to determine the constrained force at the ith contact node, the relative displacement across the contact interface is needed. In this manuscript, the second body of each contact interface is assumed to be the rigid ground. Therefore, instead of using the relative displacement, the displacement of the contact node is used.

The constrained force at these friction contact points can be obtained by employing the 3-D friction contact model. For any given displacement at the contact node, discrete simulation for the induced stick–slip friction is performed. Since analytical transition criteria are used in the simulation, it takes at most few cycles to obtain the steady state constrained force. By appropriately selecting the number of points in the discrete simulation, the steady state constrained force can be resolved into Fourier series by using the FFT algorithm:

$$\mathbf{f}_i^N = \mathbf{f}_i^N(\mathbf{u}_i) \approx \sum_{k=0}^{m} \mathbf{f}_{i,k}^N(\mathbf{u}_i) e^{jk\omega t}, \tag{21}$$

where $\mathbf{f}_{i,k}^N$ represents the magnitude and phase of the kth harmonic component of the constrained force at the ith friction contact point†. In the previous studies [3, 5–7], the even harmonic components of the response were not needed due to the assumption of contact normal load. However, in this study, the constrained force is a periodic function having both odd and even harmonic components, due to the periodically varying normal load.

These constrained forces can be considered as feedback forces that come to influence the response of the entire structure. Their effects to the motion at these p contact points can be expressed as

$$\sum_{k=0}^{m} \mathbf{u}_{i,k} e^{jk\omega t} = \sum_{k=1}^{m} \mathbf{u}_{i,k}^e e^{jk\omega t} - \sum_{k=0}^{m} \sum_{l=1}^{p} \mathbf{r}_{il,k} \mathbf{f}_{l,k}^N(\mathbf{u}_l) e^{jk\omega t}, \quad i = 1, 2, \ldots, p. \tag{22}$$

According to the Multi-Harmonic Balance Method, by equating the coefficients for each harmonic frequency, a set of non-linear algebraic equations can be obtained:

$$\mathbf{u}_{i,k} = \mathbf{u}_{i,k}^e - \sum_{l=1}^{p} \mathbf{r}_{il,k} \mathbf{f}_{l,k}^N(\mathbf{u}_l), \quad i = 1, 2, \ldots, p, \quad k = 0, 1, \ldots, m. \tag{23}$$

This set of non-linear algebraic equations has the unknown $\{\mathbf{u}_{i,k}\}$, which can be solved iteratively by using the Newton–Raphson algorithm. After knowing $\{\mathbf{u}_{i,k}\}$, the constrained force can be calculated by using equation (21), and the constrained force along with the receptance can be used to calculate the periodic response of the entire system.

4. THREE-DEGREES-OF-FREEDOM OSCILLATOR

A three-degrees-of-freedom oscillator is considered in this study to illustrate the ability of the proposed method in predicting the periodic response of structures experiencing 3-D frictional constraints. The oscillator, as depicted in Figure 3, can

† Sub-harmonic components can also be included in the approach presented in this paper. However, they are ignored in the current manuscrtipt.

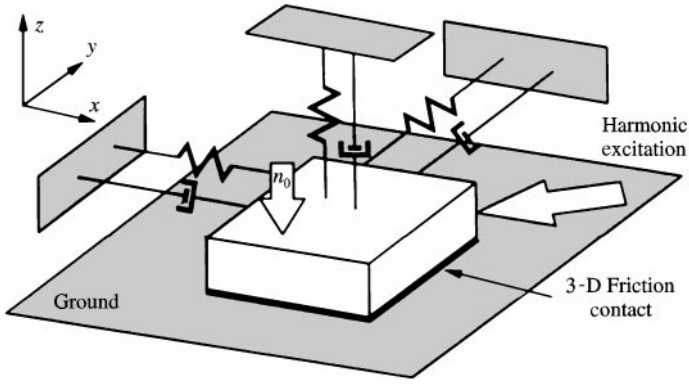

Figure 3. A three-degrees-of-freedom oscillator having a 3-D frictional constraint.

TABLE 1

Modal information of the 3-d.o.f. oscillator and the excitation

Mode	Mass	Frequency (Hz)	Damping ratio	Mode shape	Excitation
1	0·1	0·5	0·01	$(1\ 1\ 0{\cdot}8)^{\mathrm{T}}$	$1{\cdot}0 < 0^{\circ}$
2	0·1	3·0	0·01	$(-1\ 1\ 0{\cdot}6)^{\mathrm{T}}$	$1{\cdot}0 < 0^{\circ}$

move in the xyz space, and either is brought into contact with the ground by a preload n_0 or has an initial gap in between. The interface between the oscillator and the ground is modelled as a flexible Coulomb friction contact, which is shown in Figure 2. When subjected to external excitation, the xy motion of the oscillator is restricted by friction, while the z motion may cause the normal load across the interface to vary. Instead of using the conventional mass–spring–dashpot notation, this 3-d.o.f. system can be described alternatively by its modal information involving three vibration modes. It can be shown that at least two vibration modes involved in the frequency range of interest are needed to result in a response having three-dimensional periodic motion. To simplify the analysis, only two modes are considered, and the third mode is neglected from the analysis by letting its natural frequency out of the frequency range of interest. The system parameters of the 3-d.o.f. oscillator under investigation along with the harmonic modal excitation are shown in Table 1. The parameters of the friction interface used in this investigation are: $\mu = 0{\cdot}5$, $\mathbf{K_u} = diagonal[20\ 20]$, and $k_v = 20$.

4.1. PERIODIC RESPONSE

In this study, the first three harmonic components of the periodic response are included in the analysis. Under various levels of preload, the periodic responses of the 3-d.o.f. oscillator are calculated and shown in Figure 4. Since the resulting

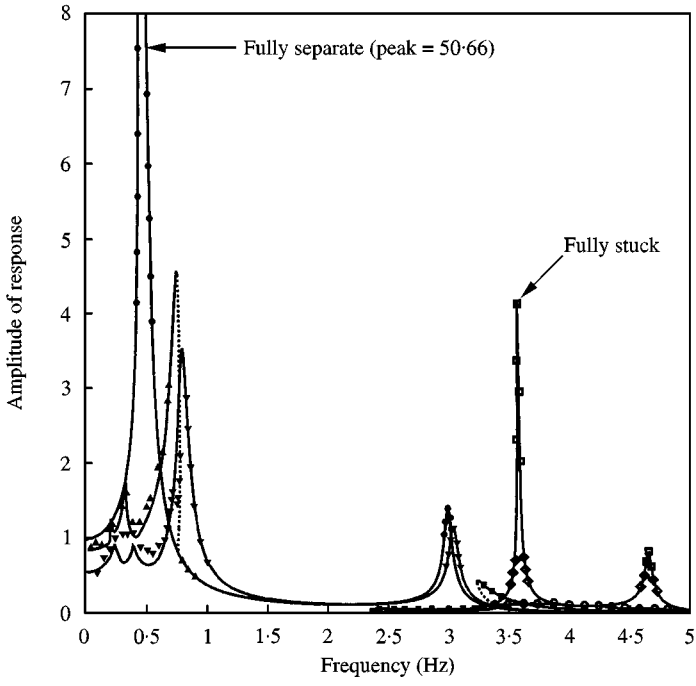

Figure 4. Periodic response of the 3-d.o.f. oscillator: ——, 3HBM; discrete data, Time Integration Method; n_0 values: ●, fully separate; ▲, −12; ▼, 0; ■, 2; ●, 5; ♦, 50; ■, fully stuck.

responses along the three axes are similar, only the amplitude of the response along the x direction is presented in the figure. It can be observed that there exist two limit cases, which are referred to as the fully separate case and fully stuck case. Both cases are linear problems because the non-linear contact force does not appear in the analysis. The fully separate case occurs when the interface has such a large initial gap that the vibrating oscillator cannot make contact with the ground. Since the contact force is not present, two resonant responses corresponding to the first two natural frequencies, 0·5, and 3·0 Hz, of the system can be clearly seen. In the opposite way, when the preload of the interface exceeds a level depending on the external excitation, the interface remains fully stuck. In this case, the friction contact does not dissipate energy but provides additional stiffness, which arises from the compliance of the interface, to the system to cause higher resonant frequencies at 3·59 and 4·66 Hz.

In between the two linear cases, the non-linear constrained force, including the stick–slip friction and the variable normal load, appears to affect the response of the system. The attenuation effect of the stick–slip friction can be clearly seen from the results. As the preload increases, the resonant response decreases until the minimum response is reached. Beyond this preload, the damping effect tends to reduce gradually towards the fully stuck case. The preload that gives the minimum response is known as the optimal preload.

Since the stick–slip friction has higher harmonic components, it is possible that the higher harmonics of the oscillator can be excited and result in internal

resonance. As can be seen in Figure 4, for example, when the preload is -12, the internal resonance can be observed at two resonant frequencies 0·33 and 0·21 Hz, where the second and third harmonics are significant. This also indicates that the even harmonic components can no longer be ignored because they may effect the accuracy in predicting the periodic response.

When only the fundamental harmonic component is considered, the forced response of the 3-d.o.f. oscillator under various levels of preload are calculated and shown in Figure 5. By comparing the predicted responses with those of the 3-terms Harmonic Balance Method, it can be observed that the single-term Harmonic Balance Method often overestimates the forced response. Furthermore, the single-term Harmonic Balance Method cannot predict the internal resonance in the forced response.

4.2. COMPARISON WITH TIME INTEGRATION METHOD

The comparison of the predicted results with those of the time integration method is also shown in Figures 4 and 5, in which the discrete data points denote the time integration solutions. All the comparisons are made in the frequency near resonance. From the results, it is apparent that the 3-terms Harmonic Balance Method can provide more accurate solutions than the single-term Harmonic Balance Method. In our previous work [12], using the single-term Harmonic

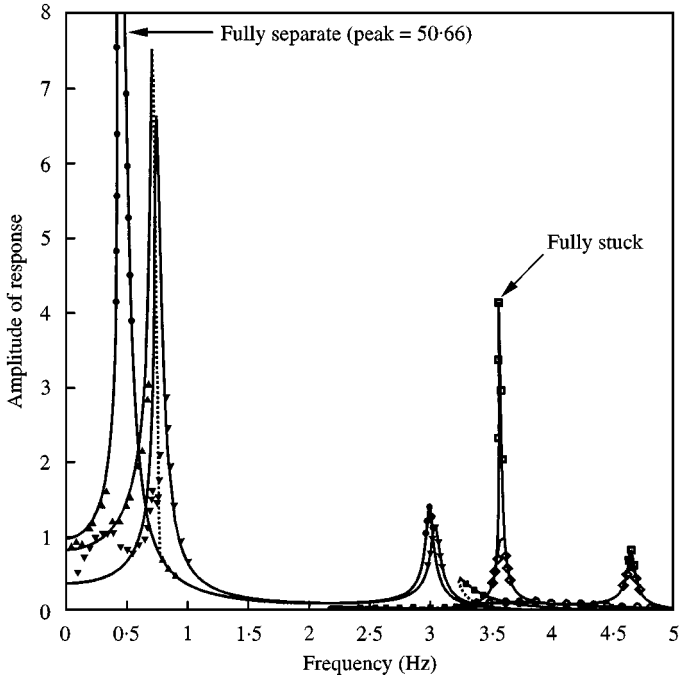

Figure 5. Periodic response of the 3-d.o.f. oscillator: ——, 1HBM; discrete data, Time Integration Method; n_0 values: ●, fully separate; ▲, -12; ▼, 0; ■, 2; ●, 5; ♦, 50; ■, fully stuck.

Balance Method, the prediction of the resonant response results in discrepancies in the cases that have either a small preload or a small gap.

In this paper, by including the super-harmonic components in the analysis, the Multi-Harmonic Balance Method can provide accurate prediction of the periodic response. Figure 6 shows the comparison of the predicted forced response by using the 1, 3 and 7-terms Harmonic Balance Method and the time integration method when the preload is 0. In this case, the super-harmonic components effect the forced response significantly within the frequency range between 0 and 1 Hz. It can be seen that the single-term Harmonic Balance Method overestimates the peak resonance by 130%, and the 3-terms Harmonic Balance Method overestimates the peak resonance by 17%. However, when the first seven harmonic components are analyzed, the predicted forced response agrees with the time integration results very well.

For further illustration, the steady state oscillation trajectories of the displacement in the x direction are compared in Figure 7 when the external excitation frequency is 0·77 Hz. It is clear that the 7-terms Harmonic Balance Method can provide very accurate prediction of the fundamental harmonic component as well as super-harmonic components. It is worth noting that the super-harmonic response of the structure may not be the major reason for the very large discrepancies in Figure 7. It is possible that small super-harmonic components can induce significant changes on the stick–slip transition that lead to large discrepancies in the prediction of the constrained forces.

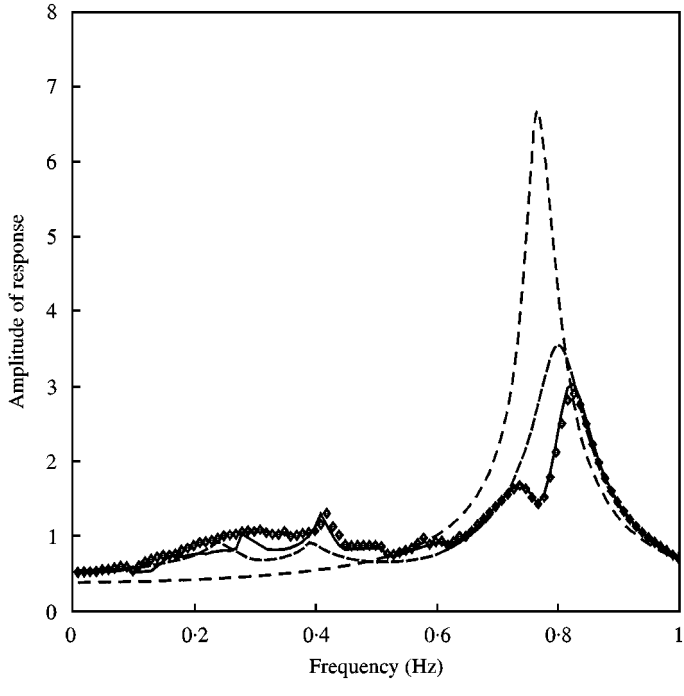

Figure 6. Comparison of periodic response of the 3-d.o.f. oscillator, $n_0 = 0°C$: ——, 7HBM; - - - -, 3HBM; – – – –, 1HBM; ♦, Time Integration Method.

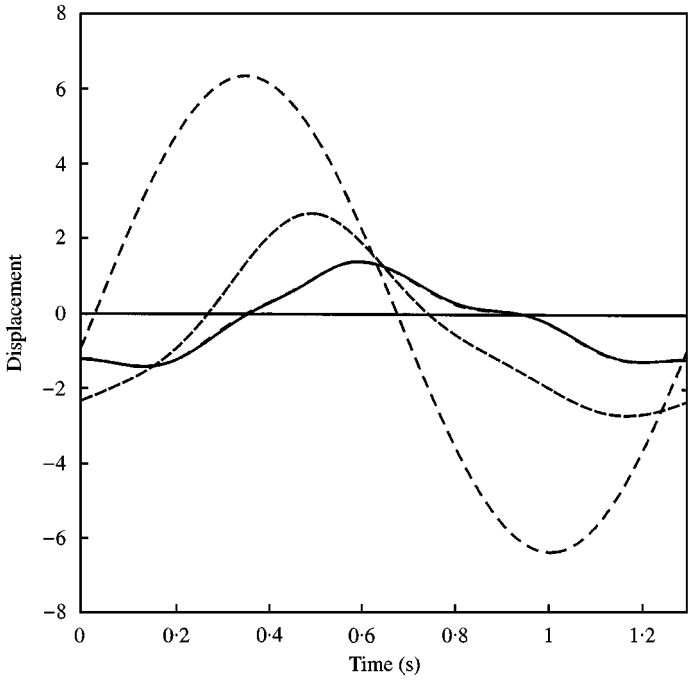

Figure 7. Comparison of periodic trajectories of the 3-d.o.f. oscillator $\omega = 0{\cdot}77$ Hz, $n_0 = 0$; ——, 7HBM; - - - -, 3HBM; – – –, 1HBM; – –; Time Integration Method.

4.3. JUMP PHENOMENON

In addition to its influence on the friction characteristic, the variable normal load can directly impose a non-linear stiffness on the system. This non-linear stiffness arises from the intermittent separation of the contact surface during the course of vibration. It has been known that this non-linearity can result in a multi-valued response that can lead to so-called "jump phenomenon" [13] and the standard continuation technique [14] can be used to obtain the multi-valued resonant response. In Figure 4, two different types of jump phenomenon can be clearly seen although the effect of the variable normal load is mixed with that of friction. The first one occurs when the interface has a moderate initial gap ($n_0 = -12$); as the amplitude of the vibratory motion increases, the interface will stay in contact for some period to impose a "hardening spring" effect on the response causing the resonant peak to bend towards higher frequencies. The other jump phenomenon, however, occurs when a moderate preload is applied ($n_0 = 2$). The increase in the amplitude of the motion causes the preloaded interface to separate, and as a result, the interface cannot provide stiffness to the system temporarily. The overall effect of the temporary separation is similar to the effect of a "softening spring" that gives rise to the response with a resonance peak bending towards lower frequencies.

Figure 8 enlarges the "spring hardening" phenomenon which occurs between 0·759 and 0·782 Hz, when the preload is -12, and compares the resonant response predicted by the 3-terms Harmonic Balance Method and the single-term Harmonic

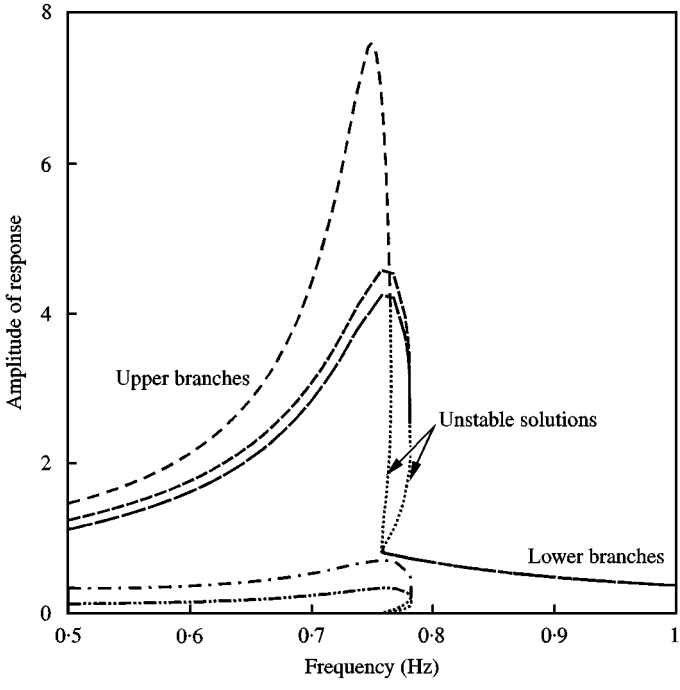

Figure 8. "Spring hardening" jump phenomenon: $n_0 = -12$: – – –, 3HBM; – – –, 1HBM; — —, 1st harmonic; –·–· 2nd harmonic; – ··– ··, 3rd harmonic.

Balance Method. It can be seen that the single-term Harmonic Balance Method overestimates the peak response by 80%. It should also be noted that one of the multiple solutions from the harmonic balance method shown as the dotted curve is unstable [13]; while separated by the unstable response, the stable response consists of two curves, which are referred to as the upper and lower branches. Figure 9 enlarges two "spring softening" phenomena when the preload is 2. The one occurs between 2·35 and 2·38 Hz is shown in Figure 9(a) and the other between 3·21 and 3·39 Hz in Figure 9(b). In this figure, the resonant response predicted by the single-term Harmonic Balance Method is compared to that by the 3-terms Harmonic Balance Method. It is found that the 3-terms Harmonic Balance Method predicts the jump phenomenon more accurately than the single-term Harmonic Balance Method, which often overestimates the resonant response at the region near jump. In addition, it can be observed that the second harmonic component can no longer be ignored because of the periodically varying normal load.

5. CONCLUSIONS

In this paper, a 3-D friction contact model is employed to predict the periodic response of structures have 3-D frictional constraints. When subjected to periodic excitation, the resulting relative motion at the friction contact interface is assumed to be periodic in the three-dimensional space. Based on the 3-D shroud contact

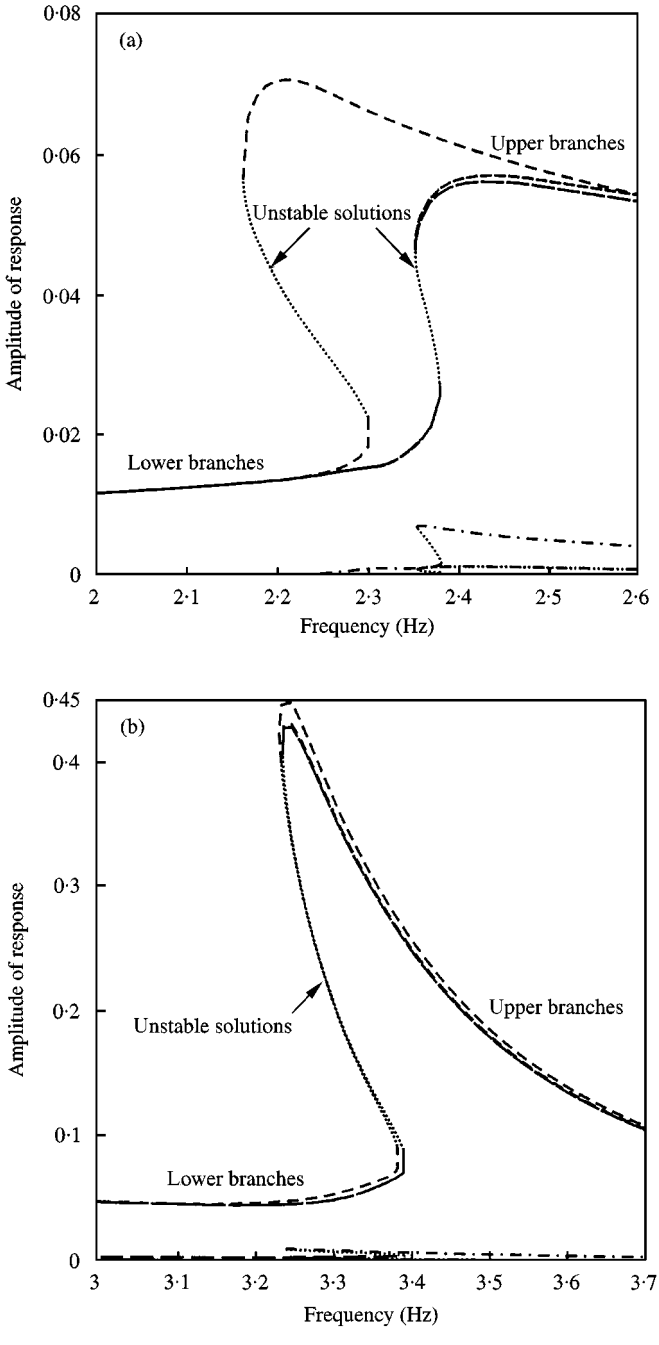

Figure 9. Two "spring softening" jump phenomena, $n_0 = 2$: (a) first spring softening jump phenomenon between 2·35 and 2·38 Hz; (b) second spring softening jump phenomenon between 3·21 and 3·39 Hz; – – – –, 3HBM; – – –, 1HBM; — —, 1st harmonic; – · – ·, 2nd harmonic; – ·· –··, 3rd harmonic.

model, analytical criteria are used to determine the transitions among sticks, slips and separations of the contact interface and are used to simulate hysteresis loops of the induced constrained force, when experiencing periodic relative motion. The constrained force can be considered as a feedback force that influences the response of the shrouded blade. By using the Multi-Harmonic Balance Method along with Fast Fourier Transform, the constrained force can be approximated by a series of harmonic functions so as to predict the periodic response of a frictionally constrained structures. Due to the periodically changing normal load, both even and odd harmonic components need to be included in the analysis.

The developed method is used to predict the periodic response of a frictionally constrained 3-d.o.f. oscillator. The predicted non-linear response shows three distinct features: (1) shifted resonant frequency due to the additional spring constant introduced by the frictional constraint, (2) damped resonant response due to the additional friction damping introduced by frictional slip, (3) multi-valued response leading to a jump phenomenon due to intermittent interface separation. The predicted results are also compared with those of the direct time integration method so as to validate the proposed method. In addition, the effect of super-harmonic components on the resonant response and jump phenomenon is examined. It was found that the single-term Harmonic Balance Method often overestimates the resonant response of a frictionally constrained structure and cannot predict the internal resonance in the forced response. It is also found that small super-harmonic components can induce significant changes on the stick–slip transition and lead to large discrepancies in the prediction of the constrained forces.

ACKNOWLEDGMENT

This material is based on work supported by the GUIde Consortium and the U.S. Air Force under contract No. F33615-96-C-2664. Any opinions, findings, and conclusions or recommendations expressed in this material are those of the authors and do not necessarily reflect the views of the GUIde Consortium or the Air Force.

REFERENCES

1. J. H. Griffin 1989 *Transactions of the American Society of Mechanical Engineers, Journal of Engineering for Power* **102**, 329–333. Friction damping of resonant stresses in gas turbine engine airfoils.
2. J. P. Den Hartog 1931 *Transactions of the American Society of Mechanical Engineers*, APM-53-9, 107–115. Forced vibration with combined Coulomb and viscous friction.
3. Y. Wang 1996 *Journal of Sound and Vibration* **189**, 299–313. An analytical solution for periodic response of elastic-friction damped systems.
4. T. M. Cameron and J. H. Griffin 1989 *Journal of Applied Mechanics* **56**, 149–154. An alternating frequency/time domain method for calculating the steady state response of nonlinear dynamic systems.
5. Y. Ren and C. F. Beards 1994 *Journal of Sound and Vibration* **172**, 593–604. A new receptance-based perturbative multi-harmonic balance method for the calculation of the steady state response of the non-linear systems

6. J. H. Wang and W. K. Chen 1993 *Journal of Engineering for Gas Turbine and Power* **115**, 294–299. Investigation of the vibration of a blade with friction damper by HBM.
7. A. A. Ferri and E. H. Dowell 1988 *Journal of Sound and Vibration* **124**, 207–224. Frequency domain solutions to multi-degree-of-freedom, dry friction damped systems.
8. J. Guillen and C. Pierre 1996 *Proceedings of the* 1996 *ASME IMECE*, Atlanta, GA, November 17–22. Analysis of forced response of dry-friction damped structural system using an efficient hybrid frequency–time method.
9. C. Pierre, A. A. Ferri and E. H. Dowell 1985 *Journal of Applied Mechanics* **51**, 958–964. Multi-harmonic analysis of dry friction damped systems using an incremental harmonic balance method.
10. C. H. Menq, J. H. Griffin and J. Bielak 1986 *Transactions of American Society of Mechanical Engineers*, *Journal of Engineering for Gas Turbines and Power* **108**, 300–305. The influence of a variable normal load on the forced vibration of a frictionally damped structure.
11. B. D. Yang and C. H. Menq 1997 *Transactions of the American Society of Mechanical Engineers*, *Journal of Engineering for Gas Turbines and Power* **119**, 958–963. Modeling of friction contact and its application to the design of shroud contact.
12. B. D. Yang and C. H. Menq 1998 *Journal of Sound and Vibration* **217**, 909–925. Characterization of 3-D contact kinematics and prediction of resonant response of structures having 3-D frictional constraint.
13. W. T. Thomson 1988 *Theory of Vibration with Applications* NJ: Englewood Cliffs, Prentice-Hall.
14. E. L. Allgower and K. Georg 1990 *Introduction to Numerical Continuation Methods.* Berlin: Springer.